ภาควิชาวิศวกรรมเหมืองแร่และวัสดุ

คณะวิศวกรรมศาสตร์

มหาวิทยาลัยสงขลานครินทร์

การสอบปลายภาค ประจำภาคการศึกษาที่ 1 ปีการศึกษา 2555

วันที่ 8 ตุลาคม 2555 เวลา 09.00-12.00 น.

วิชา 237-407 Failure Mechanics and Analysis ห้อง A401

<u>คำชี้แจงสำหรับนักศึกษา</u>

1. ข้อสอบมีจำนวน 5 ข้อ (จำนวน 2 หน้า รวมใบปะหน้านี้)
2. เอกสารประกอบข้อสอบ Case study: Case internal oxidation and intergranular fracture of carburized splined-shaft และข้อมูลอื่นๆ ที่เกี่ยวข้อง รวม 13 หน้า
3. ตอบคำถามลงในสมุดคำตอบ เขียนหมายเลขข้อให้ชัดเจน
4. สามารถนำเอกสารทุกชนิด และอุปกรณ์ช่วยสอบได้ทุกชนิด เข้าห้องสอบได้
5. คะแนนสอบครั้งนี้คิดเป็น 30 % ของคะแนนรวมทั้งหมด

<u>คำชี้แจงสำหรับกรรมการจัดทำข้อสอบ และผู้คุมสอบ</u>

1. ให้แจกสมุดคำตอบคนละ 1 เล่ม

อ . ณรงค์ฤทธ์ โทธรัตน์

ผู้ออกข้อสอบ

ข้อที่	คะแนนเต็ม	คะแนนของนักศึกษา
1	20	
2	40	
3	10	
4	20	
5	10	
คะแนนรวม	100	

แบบทดสอบการวิเคราะห์การชำรุดอย่างเป็นระบบ ปีการศึกษา 2555

I. ข้อกำหนดในการสอบ

1. สามารถนำเอกสารทุกชนิด และอุปกรณ์ช่วยสอบได้ทุกชนิด เข้าห้องสอบได้
2. จากรายงานผลการวิเคราะห์การชำรุด 1 ฉบับ

Case Study : ***Case internal oxidation and intergranular fracture of carburized splined-shaft***

ให้นักศึกษา ใช้ความรู้ ด้าน Fracture Mechanics, Systematic Failure Analysis, Heat Treatment, Metallurgy, Materials Engineering, Manufacturing Process และความรู้อื่นๆ ด้านวิศวกรรมศาสตร์ อธิบายผลการวิเคราะห์ เพื่อใช้ในการตอบข้อสอบ

3. เวลา 3 ชั่วโมง ข้อสอบ มีทั้งหมด 4 กลุ่มเป้าหมาย (Materials Analysis, Process Analysis, Failure Analysis, Management & Prevention)

II. วัตถุประสงค์ในการสอบ

เพื่อให้นักศึกษาสามารถวิเคราะห์ปัญหาทั้งระบบ นำทฤษฎี มาเชื่อมโยงกับการปฏิบัติ และประยุกต์ใช้ในการอธิบายปรากฏการณ์ที่เกิดขึ้นกับชิ้นงานจริงและมองในเชิงการบริหารและจัดการได้

เหตุการณ์สำคัญ

รถบรรทุกใช้เครื่องยนต์ดีเซล วางแผนการผลิตใช้ในประเทศ หลังจากผลิตรถยนต์ต้นแบบเสร็จ ได้ถูกนำไปทดลองวิ่งใช้งาน พบว่า Splined-shaft ซึ่งเป็นชิ้นส่วนในภายใน หลังจากใช้งาน 7 – 8 ชั่วโมง เกิดการชำรุด ผู้ผลิตจึงได้ส่งให้ มหาวิทยาลัยเป็นผู้วิเคราะห์การชำรุด

จงตอบคำถามต่อไปนี้

1. สาเหตุใดจึงต้องดำเนินการทำ Heat treatment วัสดุดังกล่าว และสาเหตุใดจึงเลือกใช้กรรมวิธี Carburizing (20 คะแนน)

2. Splined-shaft ดังกล่าวรับภาระแบบ pure torsion จงอธิบายดังต่อไปนี้

2.1 Failure mode ของ Splined-shaft คือ Mode ใด (10 คะแนน)

2.2 อธิบายความเค้นที่เกิดขึ้นบริเวณจุดขาดชำรุดด้วย Mohr's Circle (10 คะแนน)

2.3 จงเลือกทฤษฎีการชำรุดพร้อมอธิบายเหตุผลให้สอดคล้อง (20 คะแนน)

3. เหตุใดที่การเกิด Embrittlement ลึก 20 micron ของผิวรูด้านใน Splined-shaft จึงไม่ใช่สาเหตุที่ทำให้ Splined-shaft ชำรุด (10 คะแนน)

4. จุดอ่อนของการออกแบบ Splined-shaft ที่ทำให้เป็นสาเหตุหลักของการชำรุดคืออะไร และสาเหตุสำคัญที่ส่งเสริมให้ Splined-shaft เกิดการชำรุดปรากฏการณ์ใด (20 คะแนน)

5. หากนักศึกษาเป็นวิศวกรผู้ควบคุมการแก้ปัญหา และปรับปรุงการผลิต Splined-shaft ดังกล่าว มีวิธีการดำเนินการใดบ้างพร้อมเหตุผล (10 คะแนน)

ผู้ออกข้อสอบ : ณรงค์ฤทธ์ โทธรัตน์

Engineering Failure Analysis 22 (2012) 141–151

Contents lists available at SciVerse ScienceDirect

Engineering Failure Analysis

journal homepage: www.elsevier.com/locate/engfailanal

Case internal oxidation and intergranular fracture of carburized splined-shaft

Zhi-wei Yu, Xiao-lei Xu *, Zhi Yang, Yuan-yuan Li

Electromechanics and Material Engineering College, Dalian Maritime University, Dalian 116026, PR China

ARTICLE INFO

Article history:
Received 27 October 2011
Received in revised form 14 January 2012
Accepted 31 January 2012
Available online 8 February 2012

Keywords:
Splined-shaft
Carburizing
Case internal oxidation
Intergranular fracture
Stress concentration

ABSTRACT

The splined-shafts used in truck diesel engine fractured after service of merely 7–8 h. The transverse fracture occurred at the root fillet between the tooth portion and the cylinder portion. The fracture surfaces, corresponding to the carburized layer, of the failed splined-shaft and manufactured artificially show intergranular fracture features. Intergranular facets within a depth of about 20 μm from the surface were found to be associated with the oxide compounds of Cr, Mn, Si and dimples. The fracture mechanism of the splined-shaft was ductile intergranular cracking. Microstructure observation indicates intergranular internal oxidation occurred in the carburized layer to a depth of about 20 μm, in which oxide compounds of Cr, Mn, Si are along the grain boundaries. The association of intergranular oxidation pre-cracks with microstructural embrittlement promoted the premature failure of the splined-shaft. Over-short axial free length between the tooth portion and the cylinder portion enhances the degree of stress concentration, which contributes to the failure of the splined-shaft.

© 2012 Elsevier Ltd. All rights reserved.

1. Introduction

It was reported that two truck diesel engine splined-shafts fractured in service of merely 7–8 h. One of the as-received auxiliary driving assemblies containing a fractured splined-shaft is shown in Fig. 1. The failed splined-shafts are made from 20MnCr5 steel. The external surface of spline-shaft is required to be carburized. The treatment was conducted at 930 °C for 4 h, then pre-cooled at 840° for 15 min, directly quenched in an oil bath, and tempered at 180 °C for 2 h. The surface hardness is specified as HV_{10} 675–770 and the depth of carburized layer as 0.30–0.80 mm.

The pinions of splined-shaft are exposed to a surface carburizing treatment to produce high surface strength and good wear resistance. However, this treatment may strongly embrittle the pinions resulting from some carburizing defects. Specially, the intergranular brittle fracture may occur if the austenite grain boundaries are embrittled. In general, such an embrittlement is associated with high phosphorous and carbon concentration in the base steel [1], or with hydrogen absorption from the carburizing atmosphere [2]. Another surface defects of carburized steel to consider when dealing with the brittle fracture of carburized parts, is the possible formation surface intergranular oxidation, if oxygen is present in the carburizing atmosphere [3,4]. The expected microstructure near the surface of carburized steel is martensite with some amount of retained austenite. However, it is well known that gas carburizing methods are widely used. When the steel is carburized in the endothermic atmosphere, the internal oxidation will unavoidably take place in the surface layer. Oxides of alloying elements having a higher affinity for oxygen than base metal, such as elements Cr, Mn, and Si would form along the grain boundaries, and accompanied non-martensitic microstructure due to depletion of substitutional alloy elements [5,6]. Crack initiation by intergranular fracture may occur [7] to lead to premature failure of components.

* Corresponding author. Tel.: +86 0411 84729613; fax: +86 0411 84729611.
E-mail addresses: xiaoleixu.dlmu@yahoo.com.cn, xxiaolei@dlmu.edu.cn (X.-l. Xu).

1350-6307/$ - see front matter © 2012 Elsevier Ltd. All rights reserved.
doi:10.1016/j.engfailanal.2012.01.016

To determine the exact cause of failure, as-received two failed splined-shafts were subjected to detailed fractographic and metallographic examinations. They show identical fractographic and metallurgical features and failure nature. Therefore, in this paper the observation results on one of the failed splined-shafts will be presented.

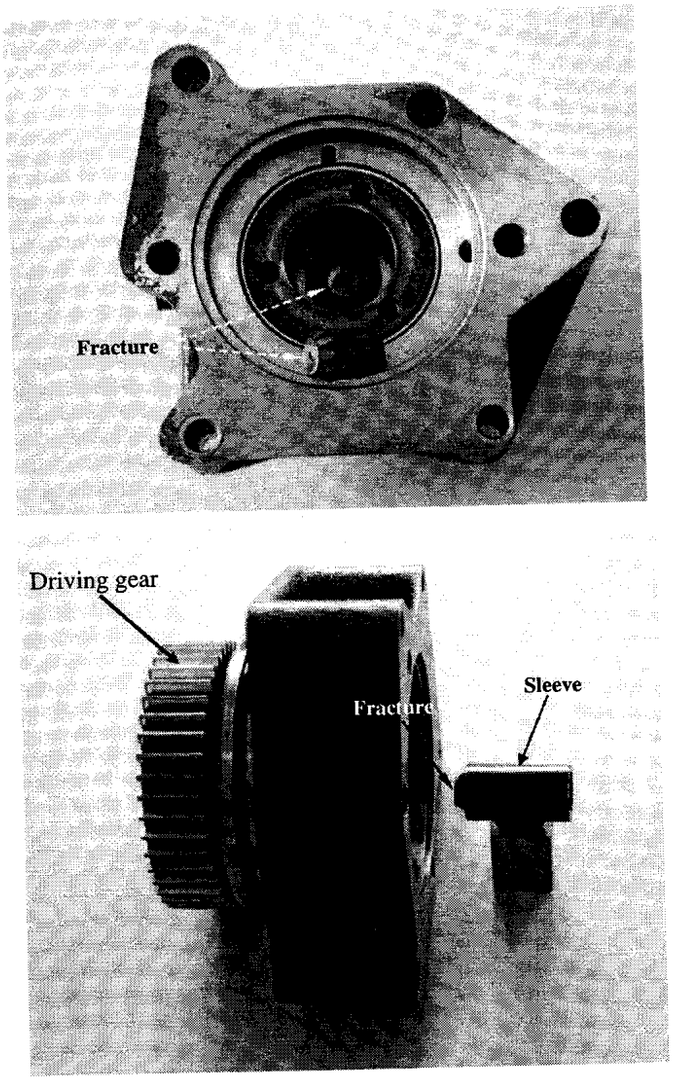

Fig. 1. Failed auxiliary driving assemble.

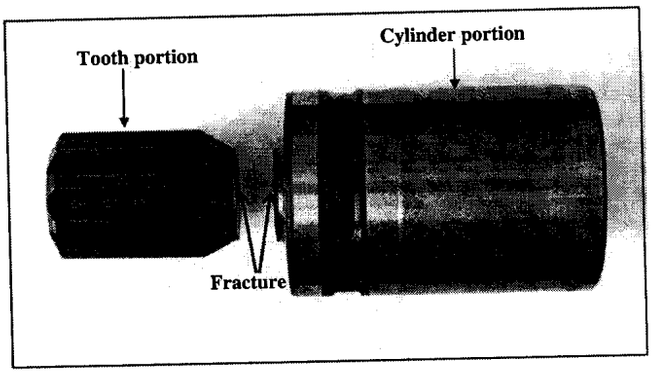

Fig. 2. Fractured splined-shaft.

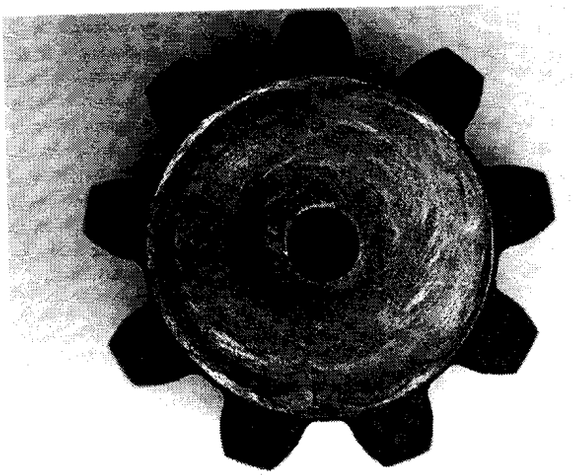

Fig. 3. Macro-fracture of splined-shaft.

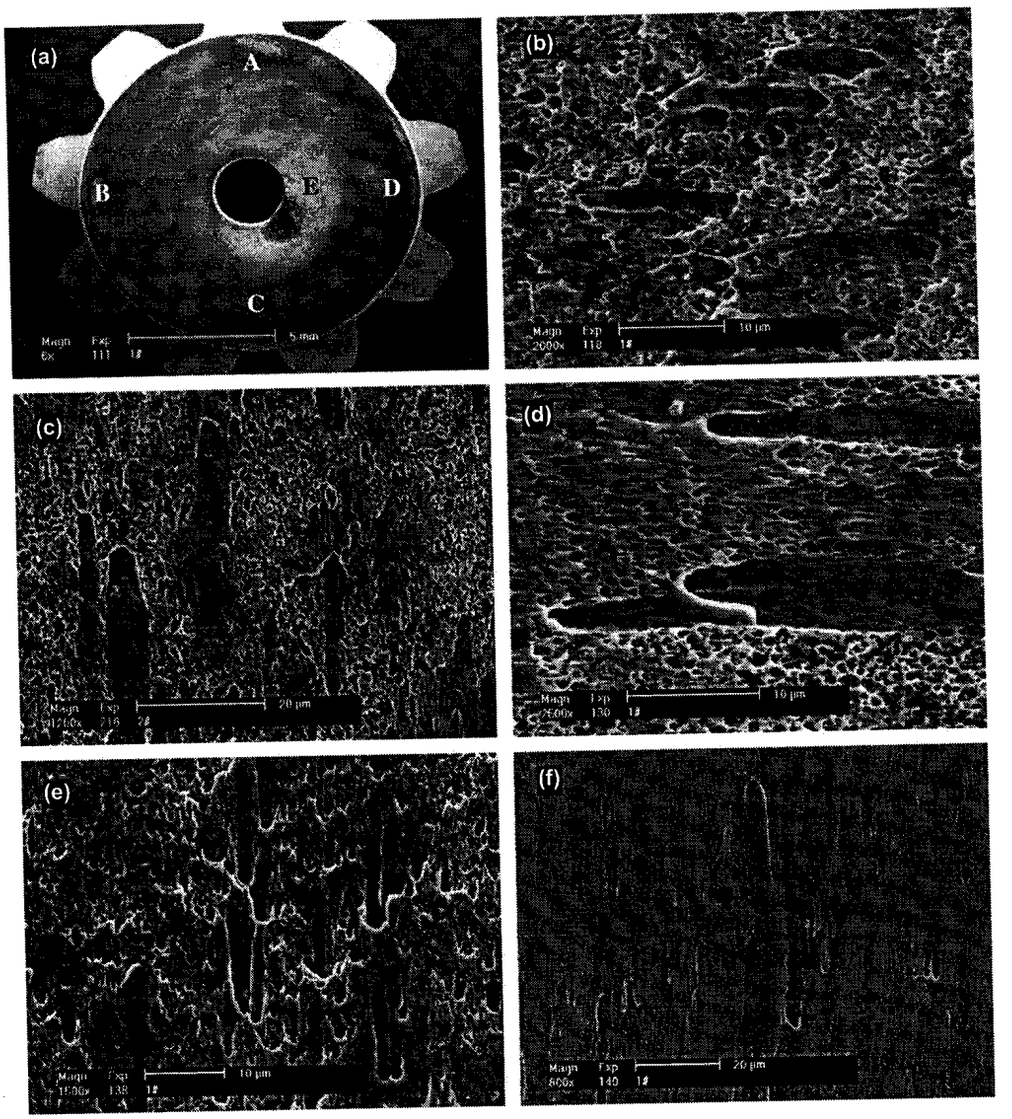

Fig. 4. SEM observation on fracture surface showing parabola dimples: (a) general view, (b) zone A, (c) zone B, (d) zone C, (e) zone D, and (f) showing scrape marks.

2. Investigation methods

The chemical composition of the splined-shaft material was determined by spectroscopy chemical analysis. The sectional microstructure was observed by scanning electron microscope (SEM) and optical microscope (OPM). The crack surfaces were observed visually and using SEM. Vickers hardness profiles from the surface to the interior in various regions were made by

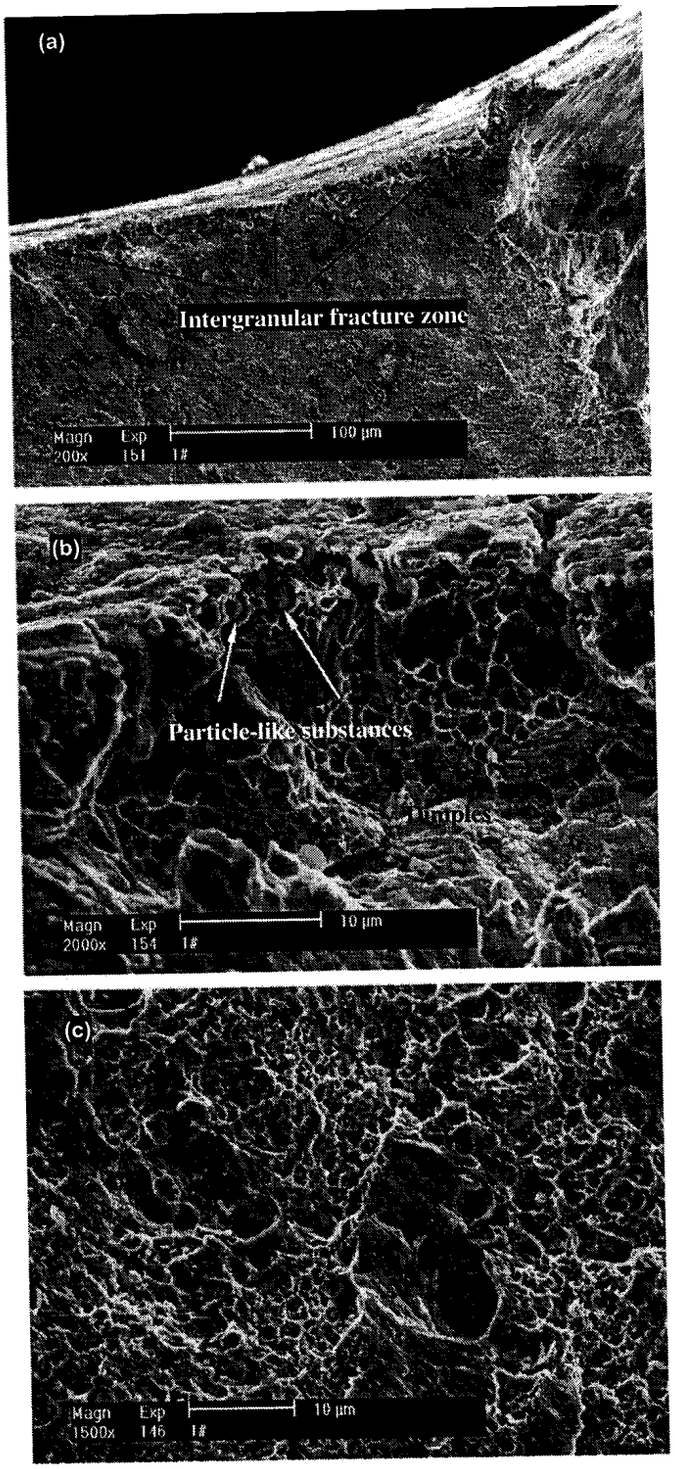

Fig. 5. SEM observation on fracture surface close to the internal hole: (a) general view on intergranular fracture region, (b) showing intergranular facets associated with dimples and precipitates, and (c) showing dimples morphology in the instantaneous region (E region in Fig. 4).

Vickers system with a load of 1000 g to determine the depth of the carburized layer. The criterion for determining case depth described in Chinese standard GB [8] is the depth of material with hardness greater than HV_1550.

3. Observation results and discussion

3.1. Visual observation on the fracture surface in service

The failed splined-shaft is shown in Fig. 2. It can be seen that the transverse fracture occurred at the root fillet between the tooth portion and the cylinder portion. The fracture surface is perpendicular to the axis of the splined-shaft and no obvious macro plastic deformation was observed. The fracture surface is relatively flat, exhibiting sliver grey tint and the located metal gloss resulting from mutual rubbing of the fracture surfaces. High-magnified observation revealed that the fracture surface close to the center hole is rough and slight convex, characterized by a "center of twist" [9] and the circular shear traces surrounding the center of twist were found on the fracture surface (Fig. 3). It is suggested that the failure mode of the splined-shaft is torsion fracture and twist final fracture zone is situated at the fringe of center hole. However, it is difficult to determine the location of crack origin and the direction of crack propagation from the macro observation.

3.2. SEM observation on the fracture surface in service

SEM observation indicates that the fracture surface exhibits generally circular parabola shallow dimples (Fig. 4). Obvious contact scrape marks along the dragged direction of parabola dimples appear in the local regions of fracture (Fig. 4f). Unfortunately, the outer periphery of fracture surface was worn severely, so fractographic features representing a carburized sur-

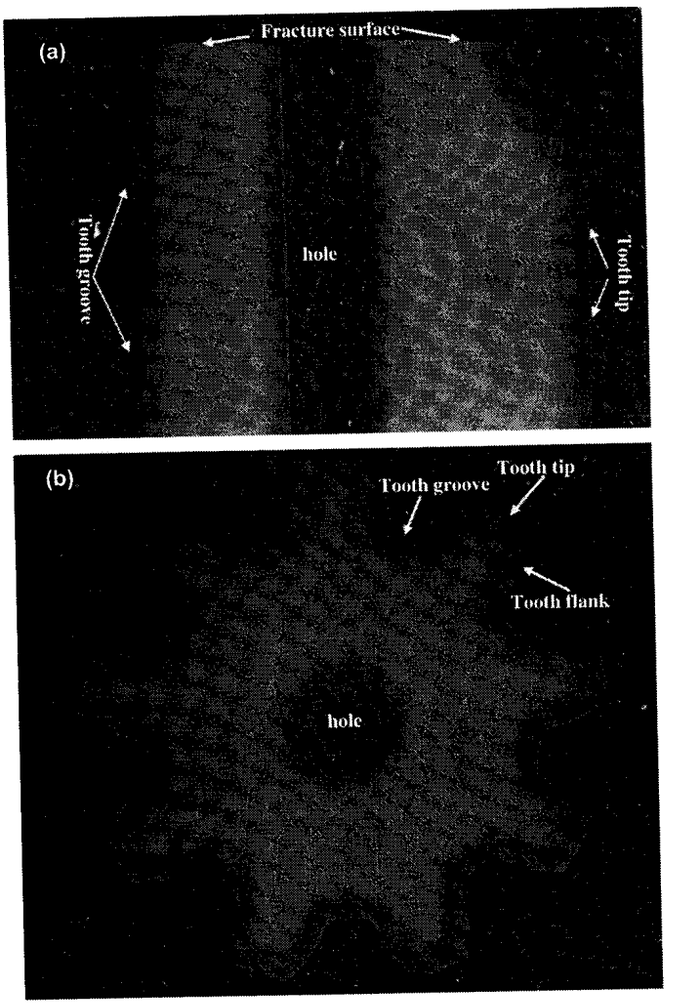

Fig. 6. Longitudinal and transverse sections of the failed splined-shaft for metallurgical examination: (a) longitudinal section and (b) transverse section.

face was not revealed. It is noted that in the located region close to the internal hole the fracture morphology is brittle, and in particular, intergranular, as shown in Fig. 5a and b and intergranular fracture extends to about 20 μm. The intergranular facets were found associated with dimples or ductile tears [10,11], and some particle-like substances were found on the intergranular facets (marked by arrows in Fig. 5b). Additionally, in the instantaneous fracture region close to the hole, deeper parabola dimples were observed (Fig. 5c).

3.3. Microstructure examination

From the macro morphology of longitudinal (through the fracture surface) and transverse sections (Fig. 6), it can be seen that the carburizing operating was conducted on the external surface of splined-shaft. Relatively thin macro case-layer was observed on the internal hole surface, suggesting that operating of preventing penetration was not performed on the internal hole surface.

Longitudinal and transverse sectional microstructure was observed by SEM. It was found that black intergranular network-like structure is presented in the carburized layer of the external surface and the internal hole surface of the splined-shaft. Representative morphology is shown in Fig. 7a and b. Precipitates were seen along the grain boundaries (Fig. 7c). As proved by EDS analysis these precipitates are oxide compounds of Cr, Mn, and Si (Fig. 8a). It is suggested that the internal oxidation near the surface occurred, which is a typical phenomenon in gas carburized steel [5]. The depth of internal oxidation is approximately 20 μm. It is highlighted that the region of internal oxidation presents grain boundary "cavities". OPM observation (Fig. 7d) indicates that a thin film of "dark component" (about 1 μm thick) alongside grain boundaries is revealed in the internal oxidation layer by slightly etching in 0.4% solution of nitric acid in alcohol [6], whose metallographic features is identical with non-martensite as described in the literatures [5–7], troosite or pearlite. The microstructure of carburized layer is mainly composed of the tempered plate-martensite and the retained austenite without intergranular network-like carbides. The microstructure of core is tempered lath-martensite.

It is noted that no decarburization was observed on the surface, in spite of presence of intergranular internal oxidation in the carburized layer. The susceptibility of different elements to oxidation can be determined by the oxidation potential P_O. Ref. [6] gives the calculated values of the internal oxidation potential for reactions and it can be seen that on heating to 930 °C in an endothermic atmosphere Si, Mn, and Cr are oxidized, while iron are not oxidized. Therefore, "external oxidation" of matrix of steel did not take place, but internal oxidation of other elements Cr, Mn, Si occurred at the boundary.

Additionally, the composition examination indicates that the splined-shaft was made from 20MnCr5 steel (Table 1).

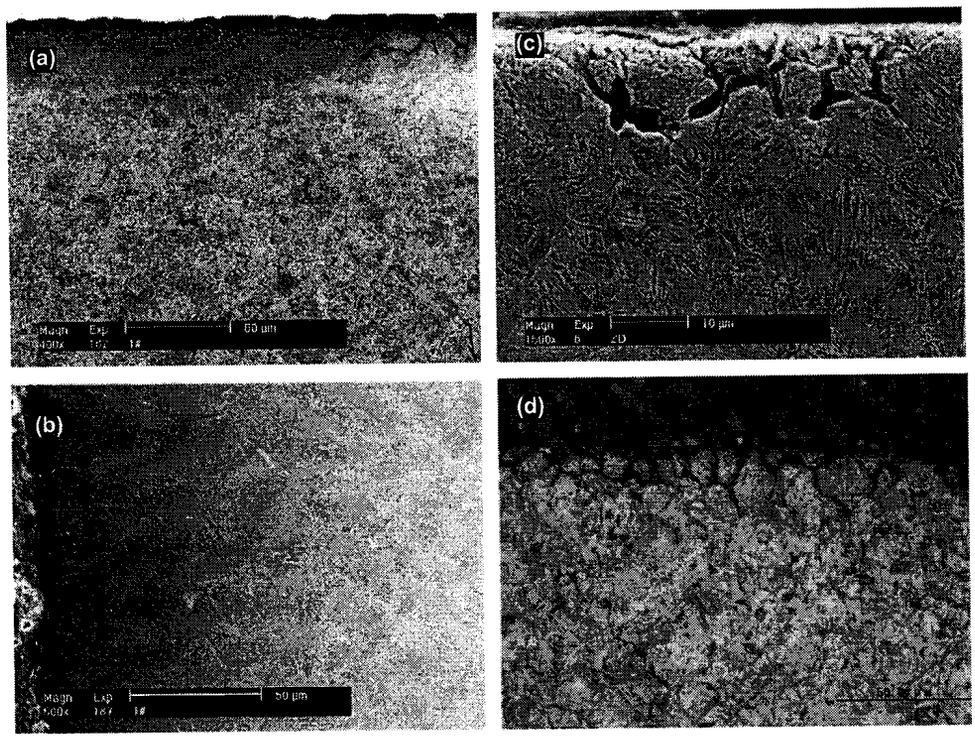

Fig. 7. Microstructure of carburized layer: (a) showing internal oxidation morphology (tip region), (b) showing of internal oxidation morphology (internal hole surface), (c) showing oxides in the grain boundaries in internal oxidation zone, and (d) showing morphology non-martensite thin film alongside the grain boundary in the internal oxidation zone by slightly etching (OPM).

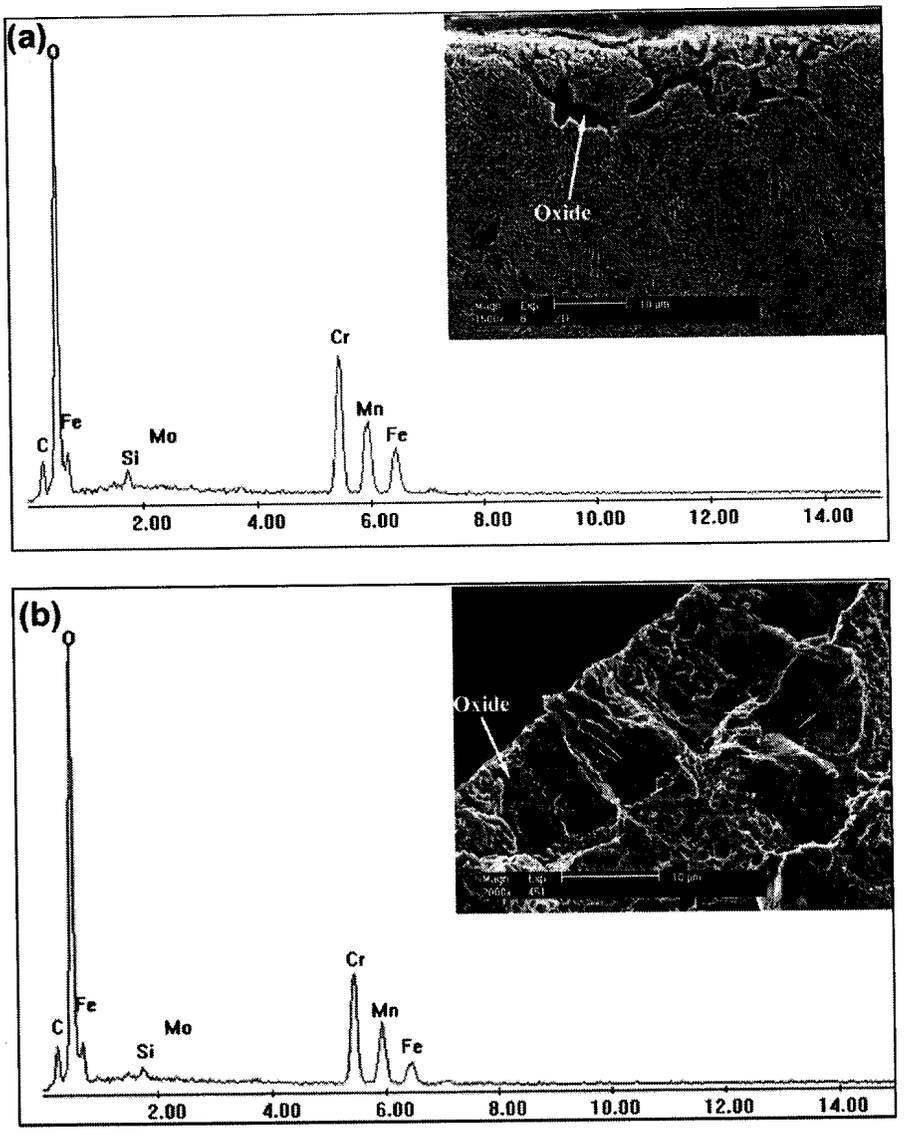

Fig. 8. EDS analysis of precipitates in the case layer and on the intergranular facets: (a) precipitates along the boundaries and (b) precipitates on the intergranular facets.

Table 1
Chemical composition of the splined-shaft (wt.%).

	C	Si	Mn	S	P	Cr	Fe
Analysised	0.18	0.24	1.25	0.011	0.016	1.30	Bal.
20MnCr5	0.17–0.22	⩽0.40	1.10–1.40	⩽0.035	⩽0.035	1.00–1.30	Bal.

3.4. Hardness examination

The surface hardness is HV_{10} 719 (average value of three readings), which is in accordance with the specified (HV_{10} 675–770). The hardness profiles in the tip, pitch line, groove and internal hole regions from the surface to the interior were measured (Fig. 9). It can be seen that the case depth of the tooth portion is generally about 0.55–0.62 mm, which corresponds to the specified (0.30–0.80 mm), and the case depth of internal hole is relatively shallow, about 0.20 mm.

3.5. Observation on the fracture surface manufactured artificially

The fracture surface of the failed splined-shaft, especially outer periphery, had been worn intensely, so the fractographic features representing a carburized surface were not revealed. However, the presence of the intergranular decohesion fea-

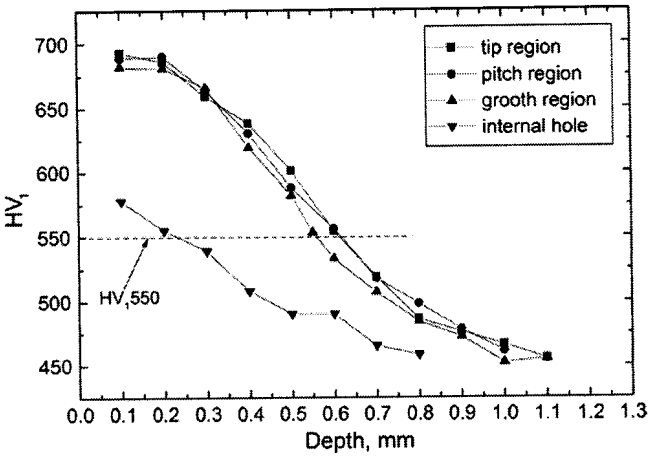

Fig. 9. Micro-hardness profiles in various region.

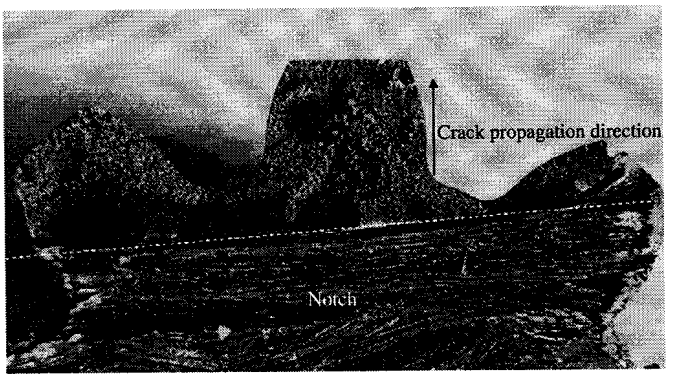

Fig. 10. Macro-fracture manufactured artificially.

tures on the fracture surface of internal hole implies some brittle failure mechanism occurred on the splined-shaft and the brittle fracture maybe relates to the case layer on the splined-shaft. To investigation the relation of intergranular fracture to the case-layer, a fracture was manufactured artificially. The semicircle transverse section was removed from the tooth portion and a transverse notch was made in the matrix by spark-cutting, then breaking off the section from the matrix toward the tooth portion to obtain identical orientation fracture with the original fracture of the failed splined-shaft. Fig. 10 shows a macrograph of fracture in the laboratory. Low-magnified SEM observation indicates that the fracture surface has a different appearance in the outer and inner regions. In the outer region of 0.7–0.8 mm from the surface the fracture surface is brittle but ductile in the tooth center (Fig. 11a). High-magnified SEM observation reveals that in the carburized area of about 0.5 mm from the surface the fracture mode is predominately intergranular (Fig. 11b). An obvious interface is revealed at the location of about 20 μm from the surface (marked in Fig. 11c). However, a close examination of Fig. 11d shows particle-like or rod-like substances at the intergranular facets. As proved by EDS analysis these substances are also oxide compounds of Cr, Mn, and Si (Fig. 8b), in accordance with the precipitates at the grain boundaries of the case layer. It is highlighted that dimples or ductile tears were observed at separated grain facets (Fig. 11d). The fractographic features are similar to those presented in the internal hole region of the failed splined-shaft. This indicates that the cracking occurred by microvoid coalescence alongside grain boundaries typical of a crack propagation by a ductile intergranular mode [10,11]. This behavior is known to results from highly localized plastic deformation within relatively "soft" zones alongside grain boundaries [12], e.g. troosite or pearlite network [5]. It is well known that the occurrence of the internal oxidation on the carburized layer can induce the formation of non-martensitic structure alongside the grain boundaries, e.g. pearlite, troosite or bainite. The appearance of dimples or ductile tears on the intergranular facets further demonstrates that a thin film of non-martensitic structure formed alongside the grain boundaries. The presence of non-martensite structure alongside grain boundaries becomes relatively "softer" than the plate martensite. In summary, the above results indicate that the fracture mechanism was ductile intergranular cracking related to precipitation of intergranular oxides. The oxide particles are not presented on the intergranular facets in subsurface, but dimples were still observed on the individual intergranular facets (Fig. 11e). The middle region of tooth is characterized by a dimpled ductile fracture (Fig. 11f).

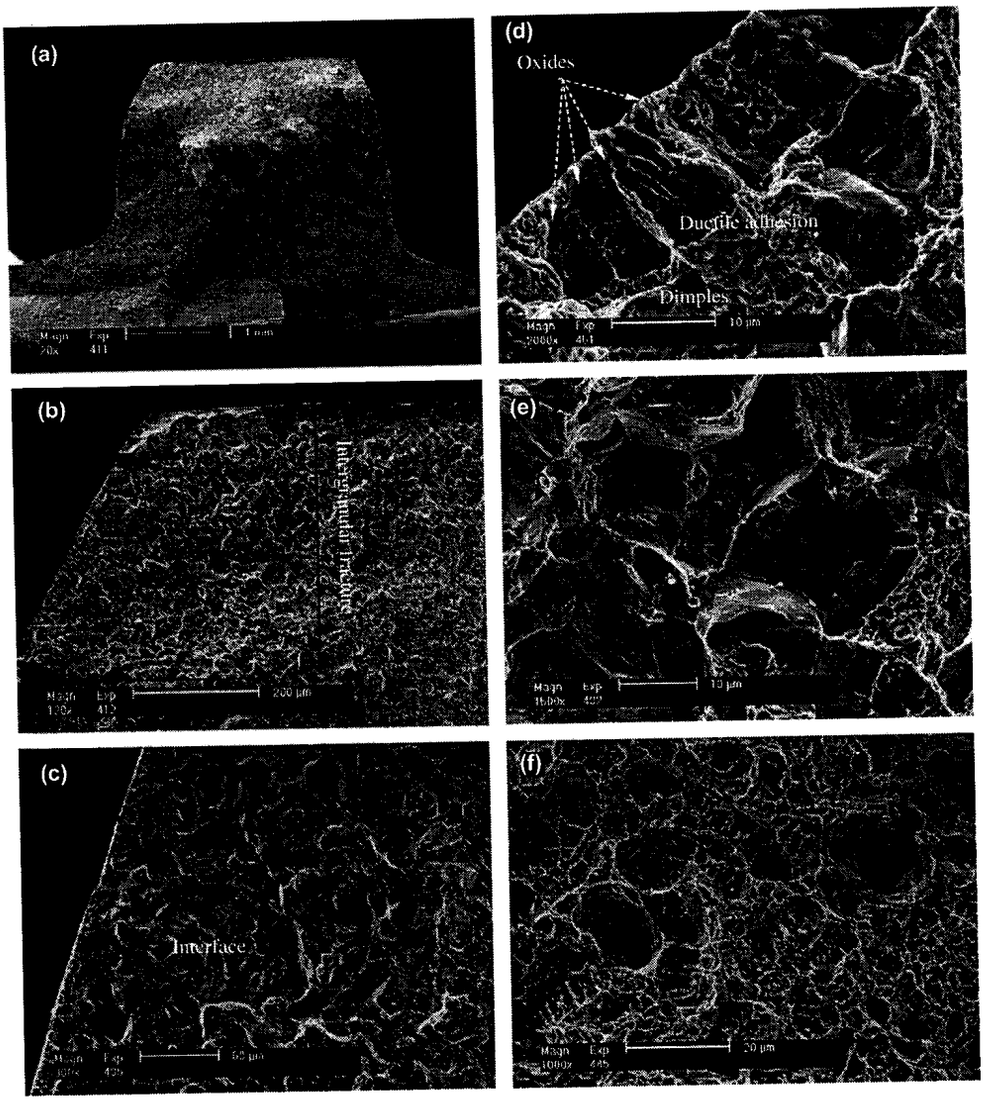

Fig. 11. SEM observation on the fracture surface prepared artificially: (a) general view, (b) showing intergranular fracture zone, (c) showing the interface corresponding to internal oxidation zone, (d) showing intergranular facets associated with the oxides and dimples, (e) showing intergranular fracture in subsurface, and (f) showing dimple morphology in the middle region.

4. Analysis of failure causes

Intergranular brittle fracture may occur on the carburized parts if the prior austenite grain boundaries are embrittled. In general, such an embrittlement is associated with a carbide net or impurity element segregation, especially phosphorous, on the prior austenite grain boundaries, or with hydrogen absorption from the carburizing atmosphere. Another microstructural feature to consider when dealing with brittle fracture of carburized components, is the possible formation of surface intergranular oxidation in gas carburized steel. From the observation and examinations in Section 3, it is inferred that the matrix microstructure, case depth, the surface hardness are within the range of the technical specification. It is noted that the chemical analysis of the splined-shaft material revealed a low phosphorous content (in agreement with the specification) and serious phosphorus segregation on the intergranular fracture surface was not probed by EDS. In order to determine if impurity segregation P associated with the grain boundary fracture noted on the carburized layer, an Auger analysis should be performed [13]. In present case, the intergranular facets associated with "ductile tear" are presented only within about 20 μm depth from the surface, which is just corresponding to the internal oxidation depth in a case layer. Therefore, in present case the intergranular embrittlement fracture should be more closely related to the presence of internal oxidation defect in the case layer and the structure anomaly be regarded as a kind of weakened zone at the surface of carburized steel. Phosphorus segregation in the embrittlement process did not act a major role.

The internal oxidation propagated preferentially along the prior-austenitic grain boundaries, presenting intergranular precipitation of oxides in the case layer. The present results also indicate that the formation of grain boundary "cavities"

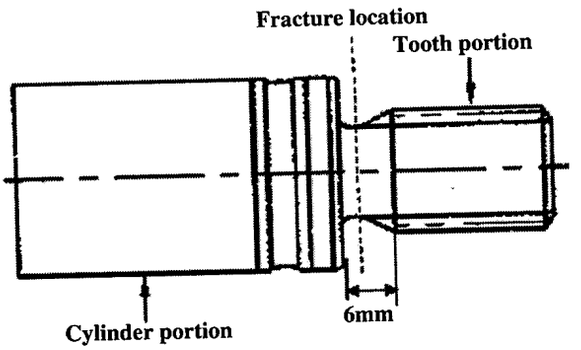

Fig. 12. The scheme of splined-shaft.

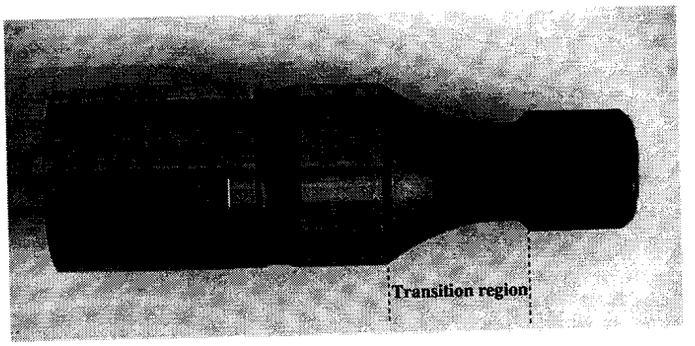

Fig. 13. Splined-shaft with suitable transition between the tooth and the shaft.

associated with the intergranular oxidation. Grain boundary "cavities" promotes that crack initiation and propagation. Finally, the intense intergranular oxide precipitates promoted the microstructural embrittlement of in the case layer, which associated with the presence of oxidation pre-cracks, lead to the brittle fracture during the service. The fractographic results confirmed that cracking followed initially the intergranular oxidation path until a depth of approximately 20 μm.

In service, the splined-shaft bears torsion load. The torsion shear stress increases with the radius along the radial of the shaft. The outmost surface of the splined-shaft bears greater shear stress. Literature indicates that cracks usually form 45° under torsional nature of loading imposed a component [14,15], while, the failed splined-shaft is not in the instance. The tooth end of splined-shaft is fully bound up by the sleeve (see Fig. 1) and the shaft end is fixed tightly in the internal hole of driving gear. From the design construction of the splined-shaft, the axial free length is relatively short (merely 6.0 mm at the fillet, see in schematic diagram of Fig. 12), equivalent to a pure notch in construction. Additionally, due to the presence of circular intergranular micro-cracks on the outer surface of the splined-shaft, the crack would propagate along the radial rather than propagating typically along the direction of 45° to the axial. At last the transverse fracture formed.

It should be pointed that the presence of intergranular internal oxidation in the case layer is not enough to cause the splined-shaft to rupture prematurely. However, in combination with greater stress concentration at the fracture location resulting from over-short axial free length between the tooth portion and the cylinder portion, the probability of such an event is considerably increased. Similar failure did not occur on another type of splined-shaft which have a suitable transition between the tooth and the cylinder (Fig. 13), despite of occurrence of internal oxidation in the case-layer.

5. Conclusions

(1) The failed splined-shaft is made of 20MnCr5 steel. The surface hardness and the case depth correspond to the specification.
(2) Internal oxidation phenomenon occurred on the carburized splined-shaft to lead to the formation of intergranular oxides of Cr, Mn, Si enveloping a "soft" zone of non-martensitic structure alongside the grain boundaries of the carburized layer. The formation of grain boundary "cavities" associated with the intergranular oxidation. Grain boundary "cavities" promotes that crack initiation and propagation.
(3) The fracture mechanism of the splined-shaft was ductile intergranular cracking. The premature failure of the splined-shaft was promoted by the occurrence of intergranular internal oxidation.
(4) Presence of intergranular internal oxidation in the case layer is not enough to cause the shaft to rupture prematurely. However, in combination with greater stress concentration at the fracture location resulting from over-short axial free length between the tooth portion and the cylinder portion, the probability of such an event is considerably increased.

Recommendations

(1) Exchange the material of splined-shaft and select the steels containing alloy elements (e.g. Mo, Ni) unsusceptible for internal oxidation. Reduce the content of gases containing oxygen in the furnace.
(2) Improve the design of the splined-shaft and obtain a suitable transition between the tooth portion and shaft portion to decrease the degree of stress concentration.

References

[1] Ando Tehchi, Krauss George. The effect of phosphorus content on grain boundary cementite formation in AISI 52100 steel. Metall Trans 1981;12A:1283–90.
[2] Kim Hyung-jun, Kweon Young-Gak. High cycle fatigue behavior of gas-carburized medium carbon C–Mo steel. Metall Trans 1996;27A:2557–64.
[3] Straffelini G, Versari L. Brittle intergranular fracture a tread: the role of carburizing treatment. Eng Fail Anal 2009;16:1448–53.
[4] Naito Takeshi, Used Hideo, Kikuchi Masao. Fatigue behavior of carburized steel with internal oxides and nonmartensitic microstructure near the surface. Metall Trans 1984;15A:1431–6.
[5] Colombo RL, Fusani F, Lamberto M. On the soft layer in carburized gears. J Heat Treat 1983;3:126–8.
[6] Koslovskii IS, Kalinin AT, Novokava AJa, Lebedova EA, Feofanova AI. Internal oxidation during case-hardening of steels in endothermic atmospheres. Metal Sci Heat Treat 1967(3 and 4):157–61.
[7] Asi Osman, Can Ahmet Cetin, Pineault James, Belassel Mohammed. The relationship between case depth and bending fatigue strength of gas carburized ASE 8620steel. Surf Coat Technol 2007;201:5979–87.
[8] Determination of carburized depth and metallurgic examination of carburizing structure. China Standard. GB9450; 1994 [in Chinese].
[9] Varin JD. Fracture characteristics of steering gear sector shafts. Pract Fail Anal 2002;2:65–9.
[10] Tawancy HM. Degradation of mechanical strength of pyrolysis furnace tubes by high-temperature carburization in a petrochemical plant. Eng Fail Anal 2009;16:2171–8.
[11] Tawancy HM. Failure of a furnace outlet pipe in a benzene plant by internal oxidation due to improper welding practice. Eng Fail Anal 2009;16:2179–85.
[12] ASM handbook, Fractography, vol. 12. Materials Park (Ohio): ASM International; 1987. p. 112.
[13] Krauss George. The microstructure and fracture of a carburized steel. Metall Trans 1978;9:1527–35.
[14] Metal Handbook. Fractography and atlas of fractographs, 8th ed., vol. 9. Metal Park (OH): American Society for Metals;1974. p. 445.
[15] Jha Abbay K, Sreekumar K, Mittal MC. Metallurgical studies on a failed EN19 steel shear pin. Eng Fail Anal 2008;15:922–30.

Figure A–15–15

Grooved round bar in torsion. $\tau_0 = Tc/J$, where $c = d/2$ and $J = \pi d^4/32$.

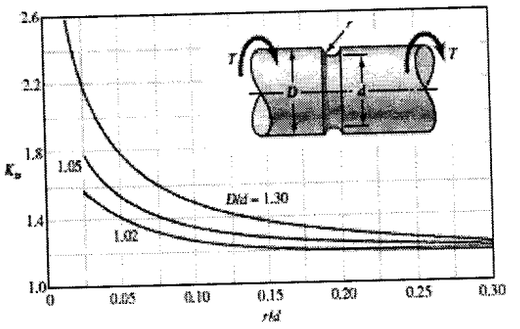

Figure A–15–8

Round shaft with shoulder fillet in torsion. $\tau_0 = Tc/J$, where $c = d/2$ and $J = \pi d^4/32$.

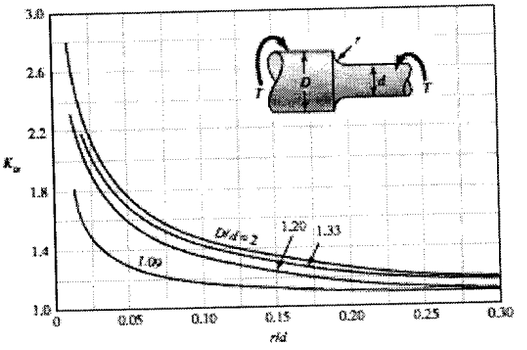

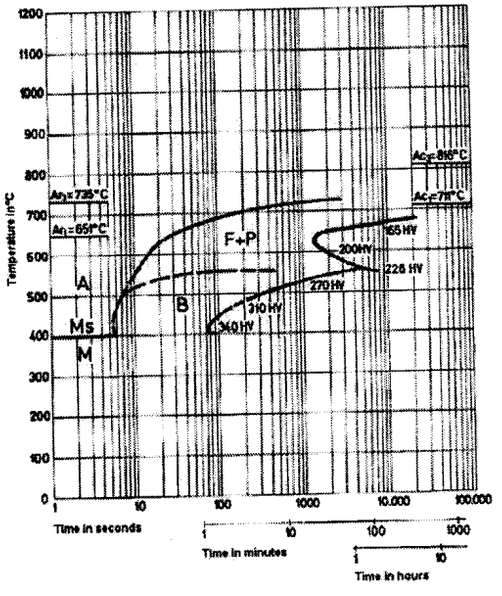

Time-Temperature Transformation (TTT) Diagram

Of 20MnCr 5

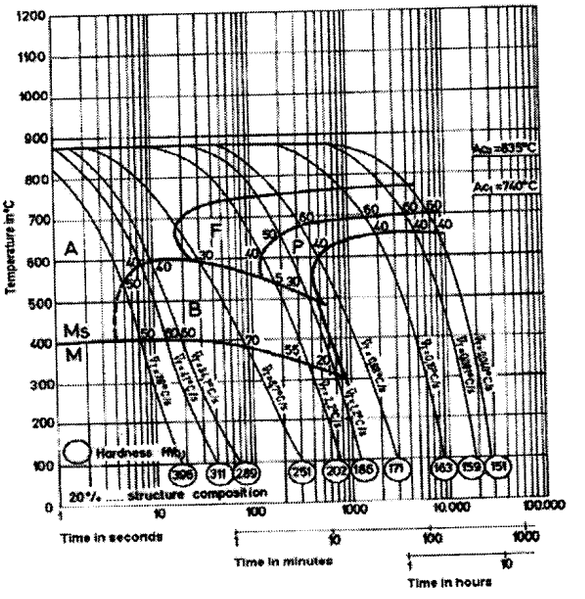

Continuous Cooling Transformation (CCT) Diagram

Of 20MnCr 5

Hardness of martensite

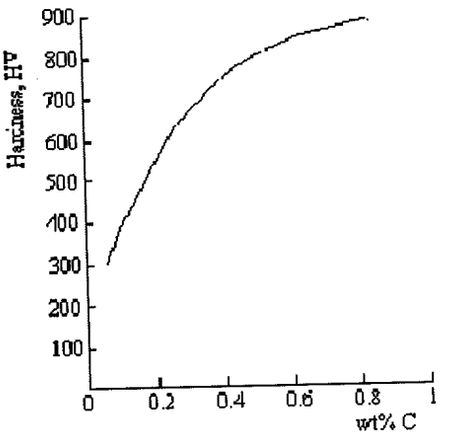

Alloy additions affect M_s & M_f

hardness of martensite **only** a function of %C

0.2%C – 50 Rc

0.4%C – 58Rc

0.8%C – 65 Rc (2000 Mpa)

Table 7 Effect of carbon concentration and % martensite on the as-quenched hardness of steel

Carbon, %	Hardness, HRC				
	99% M	95% M	90% M	80% M	50% M
0.10	38.5	32.9	30.7	27.8	26.2
0.12	39.5	34.5	32.3	29.3	27.3
0.14	40.6	36.1	33.9	30.8	28.4
0.16	41.8	37.6	35.3	32.3	29.5
0.18	42.9	39.1	36.8	33.7	30.7
0.20	44.2	40.5	38.2	35.0	31.8
0.22	45.4	41.9	39.6	36.3	33.0
0.24	46.6	43.2	40.9	37.6	34.2
0.26	47.9	44.5	42.2	38.8	35.3
0.28	49.1	45.8	43.4	40.0	36.4
0.30	50.3	47.0	44.6	41.2	37.5
0.32	51.5	48.2	45.8	42.3	38.5
0.34	52.7	49.3	46.9	43.4	39.5
0.36	53.9	50.4	47.9	44.4	40.5
0.38	55.0	51.4	49.0	45.4	41.5
0.40	56.1	52.4	50.0	46.4	42.4
0.42	57.1	53.4	50.9	47.3	43.4
0.44	58.1	54.3	51.8	48.2	44.3
0.46	59.1	55.2	52.7	49.0	45.1
0.48	60.0	56.0	53.5	49.8	46.0
0.50	60.9	56.8	54.3	50.6	46.8
0.52	61.7	57.5	55.0	51.3	47.7
0.54	62.5	58.2	55.7	52.0	48.5
0.56	63.2	58.9	56.3	52.6	49.3
0.58	63.8	59.5	57.0	53.2	50.0
0.60	64.3	60.0	57.5	53.8	50.7

M, martensite